

Article

Acid-Sensing Ion Channel 1a Contributes to the Prefrontal Cortex Ischemia-Enhanced Neuronal Activities in the Amygdala

Gyeongah Park ¹, Qian Ge ¹, Zhen Jin ¹ and Jianyang Du ^{1,2,*}

¹ Department of Anatomy and Neurobiology, University of Tennessee Health Science Center, Memphis, TN 38163, USA

² Neuroscience Institute, University of Tennessee Health Science Center, Memphis, TN 38163, USA

* Correspondence: jdu15@uthsc.edu; Tel.: +1-901-448-3463

Abstract: Following a stroke, the emergence of amygdala-related disorders poses a significant challenge, with severe implications for post-stroke mental health, including conditions such as anxiety and depression. These disorders not only hinder post-stroke recovery but also elevate mortality rates. Despite their profound impact, the precise origins of aberrant amygdala function after a stroke remain elusive. As a target of reduced brain pH in ischemia, acid-sensing ion channels (ASICs) have been implicated in synaptic transmission after ischemia, hinting at their potential role in reshaping neural circuits following a stroke. This study delves into the intriguing relationship between post-stroke alterations and ASICs, specifically focusing on postsynaptic ASIC1a enhancement in the amygdala following prefrontal cortex (PFC) ischemia induced by endothelin-1 (ET-1) injection. Our findings intriguingly illustrate that mPFC ischemia not only accentuates the PFC to the amygdala circuit but also implicates ASIC1a in fostering augmented synaptic plasticity after ischemia. In contrast, the absence of ASIC1a impairs the heightened induction of long-term potentiation (LTP) in the amygdala induced by ischemia. This pivotal research introduces a novel concept with the potential to inaugurate an entirely new avenue of inquiry, thereby significantly enhancing our comprehension of the intricate mechanisms underlying post-stroke neural circuit reconfiguration. Importantly, these revelations hold the promise of paving the way for groundbreaking therapeutic interventions.



Citation: Park, G.; Ge, Q.; Jin, Z.; Du, J. Acid-Sensing Ion Channel 1a Contributes to the Prefrontal Cortex Ischemia-Enhanced Neuronal Activities in the Amygdala. *Brain Sci.* **2023**, *13*, 1684. <https://doi.org/10.3390/brainsci13121684>

Academic Editor: Aleksandra Dugandžić

Received: 3 November 2023

Revised: 29 November 2023

Accepted: 2 December 2023

Published: 7 December 2023



Copyright: © 2023 by the authors. Licensee MDPI, Basel, Switzerland. This article is an open access article distributed under the terms and conditions of the Creative Commons Attribution (CC BY) license (<https://creativecommons.org/licenses/by/4.0/>).

Keywords: cerebral ischemia; stroke; oxygen-glucose deprivation; acid-sensing ion channels; ASIC1a; prefrontal cortex; amygdala; brain circuits; endothelin-1; depression-like behaviors; synaptic transmission and plasticity; long-term potentiation

1. Introduction

Anxiety disorders and depression occur in 24% and 29–33% of stroke patients, respectively [1], preventing post-stroke rehabilitation and functional outcomes and increasing mortality. Despite the critical consequences, post-stroke anxiety and depression remain poorly understood and treated. Thus, understanding the mechanisms of post-stroke anxiety and depression has important implications for post-stroke outcomes and rehabilitation and may decrease mortality.

After a stroke, spontaneous recovery occurs through brain remapping [2,3]. Newly developed brain circuits lead to different behavioral patterns and new response strategies to recover performance. The neuroplasticity observed in the brain after a stroke might either accelerate recovery or lead to unexpected behavioral changes resulting in emotional symptoms such as anxiety and depression [4]. Although the precise mechanisms by which brain ischemia causes alterations of neuronal activity that result in anxiety- and depression-like behaviors remain poorly understood, we suspect that they most likely involve disrupted neural connections. Neuronal functions in the core and peri-infarct areas as well as the remote brain regions they connect to are disturbed after cerebral ischemia [2]. Ischemia-induced infarction in a surface brain region may affect how it projects

to the amygdala, which is crucial for the development of anxiety- and depression-like behaviors in mice. Additionally, the increased excitatory neuronal activity in the amygdala is what causes anxiety and depression-like behaviors [5]. The amygdala generally does not experience direct infarction from mild to moderate cerebral ischemia [6], suggesting that the infarction-induced projection to the amygdala may be crucial for the ischemia-induced anxiety- and depression-like behaviors.

During a stroke and brain ischemia, reduced blood flow prevents the clearance of carbon dioxide, leading to the accumulation of lactic acid in the ischemic brain [7,8]. The brain pH in the infarction sites typically decreases to 6.5–6.0 during ischemia and can be reduced to below 6.0 during severe ischemia [7–9]. This ischemic acidosis can lead to neurological deficits [8–11]. In contrast, protons (H^+) can also function as neurotransmitters that signal through postsynaptic receptors called ASICs. ASICs play key roles in neurotransmission and synaptic plasticity in the amygdala, a critical site for the formation of emotional behaviors as well as depression and anxiety [12–15]. Six ASIC proteins have been identified (ASIC1a, ASIC1b, ASIC2a, ASIC2b, ASIC3, and ASIC4). They are members of the degenerin/epithelial sodium (Na^+) channel family. ASICs assemble as homo- or hetero-trimers to form H^+ -gated, voltage-insensitive, Na^+ - and calcium (Ca^{2+})-permeable channels that are activated by extracellular H^+ [16,17]. As a primary target of reduced brain pH in ischemia, ASIC1a enhances neuronal injury by directly or indirectly increasing cellular Ca^{2+} influx [18]. ASICs also contribute to amygdala-dependent anxiety- and depression-like behaviors [13,15], which are commonly observed after a stroke.

Under physiological conditions, two major counteracting processes control brain pH. Briefly, the utilization of glucose in neuron and glia metabolism generates CO_2 , and/or lactic acid, which results in an acidic pH shift. Counteracting the acidosis, an enhancement of neural activity causes an increase in local blood flow that facilitates the clearance of CO_2 , leading to local alkaline pH shifts [19]. During a stroke and brain ischemia, oxygen depletion in the brain forces the utilization of glucose towards anaerobic glycolysis, and the reduced blood flow prevents the clearance of CO_2 . Consequently, the accumulation of lactic acid as a byproduct of glycolysis and H^+ produced by ATP hydrolysis causes the pH to decrease in the ischemic brain [7,8]. Brain pH typically falls to 6.5–6.0 during ischemia and can fall below 6.0 during severe ischemia [7–9]. Ischemic acidosis can then lead to neurological deficits [8–11]. In addition, the rapid dynamics of metabolism and CO_2 clearance suggest that physiological changes in brain pH may have significant consequences for behavior, learning, and memory [19,20]. An intriguing idea that has emerged from studies of pH-dependent alterations in excitability is that highly localized pH transients might play a signaling role in neuronal communication. Changes in neuronal excitability and synaptic plasticity may include a significant component mediated by a pH shift [21], and H^+ may function as a ligand to effect these changes. However, how brain ischemia acidosis alters neuronal circuits and influences synaptic transmission and memory is not known.

Testing these novel concepts is expected to open a new area of inquiry and will have a substantial impact on our understanding of the mechanisms that underlie post-stroke neuronal deficits. Finally, this work will lay the foundation for the development of novel therapies for many post-stroke behavioral deficits.

2. Materials and Methods

2.1. Mice

For our experiment, we used both male and female mice between 10–14 weeks of age. Mice were derived from a congenic C57BL/6 background including wild-type (WT) and ASIC1a knockout ($ASIC1a^{-/-}$). The C57BL6 mice were ordered from the Jackson Laboratory and the $ASIC1a^{-/-}$ mice were gifted from Dr. Michael Welsh's laboratories at the University of Iowa. All mice were maintained in our animal facilities. Experimental mice were maintained on a standard 12-h light-dark cycle and received standard chow and water ad libitum. Animal care and procedures met the National Institutes of Health

standards. The University of Tennessee Health Science Center Laboratory Animal Care Unit (Protocol #19-0112) and the University of Toledo Institutional Animal Care and Use Committee (Protocol #108791) approved all procedures.

2.2. ET-1-Induced Brain Ischemia Model and Chemical Infusion

For the cannula placement procedure, mice were anesthetized with isoflurane through an anesthetic vaporizer and secured to the stereotaxic instrument, and a cannula made from a 25-gauge needle was inserted bilaterally into the medial prefrontal cortex (mPFC) (relative to bregma: +2.0 mm anterior–posterior; +0.5 mm mediolateral; –2.4 mm dorsoventral). Dental cement secured the cannula and bone anchor screw in place. Mice recovered for 4–5 days before any subsequent testing was carried out. A 10 μ L Hamilton syringe connected to a 30-gauge injector was inserted 1 mm past the cannula tip to inject anisomycin (diluted in 1 μ L artificial cerebrospinal fluid (ACSF), a pH 7.3) over 5 s. The injection sites were mapped post-mortem by sectioning the brain (10 μ m coronal) and performing cresyl violet staining.

2.3. Brain Slice Preparation and Patch-Clamp Recording of Amygdala Pyramidal Neurons

Ten minutes after the memory retrieval experiment ended, mice were euthanized with overdosed isoflurane, and whole brains were dissected into a pre-oxygenated (5% CO₂ and 95% O₂) ice-cold high sucrose dissection solution containing (in mM): 205 sucrose, 5 KCl, 1.25 NaH₂PO₄, 5 MgSO₄, 26 NaHCO₃, 1 CaCl₂, and 25 glucose [22]. A vibratome sliced brains coronally into 300 μ m sections that were maintained in normal ACSF containing (in mM) 115 NaCl, 2.5 KCl, 2 CaCl₂, 1 MgCl₂, 1.25 NaH₂PO₄, 11 glucose, 25 NaHCO₃ bubbled with 95% O₂/5% CO₂, and a pH 7.35 at 20 °C–22 °C. Slices were incubated in the ACSF at least 1 h before recording. For the experiments, individual slices were transferred to a submersion–recording chamber and were continuously perfused with the 5% CO₂/95% O₂ solution (~3.0 mL/min) at room temperature (20 °C–22 °C). In some experiments, the regular ACSF was replaced by an oxygen–glucose deprivation (OGD, glucose-free) ACSF containing (in mM): 115 NaCl, 2.5 KCl, 2 CaCl₂, 1 MgCl₂, 1.25 NaH₂PO₄, 25 NaHCO₃ bubbled with 95% N₂/5% CO₂, and a pH 7.35 at 20 °C–22 °C. The OGD incubation time was indicated in each experiment.

As we described previously [22], pyramidal neurons in the lateral amygdala were studied using whole-cell patch-clamp recordings. The pipette solution containing (in mM): 135 KSO₃CH₃, 5 NaCl, 10 HEPES, 4 MgATP, 0.3 Na₃GTP, and 0.5 K-EGTA (mOsm = 290, adjusted to a pH 7.25 with KOH). The pipette resistance (measured in the bath solution) was 3–5 M Ω . High-resistance (>1 G Ω) seals were formed in voltage-clamp mode. Picrotoxin (100 μ M) was added to the ACSF throughout the recordings to yield excitatory responses. In the AMPAR-current rectification experiments, we applied D-APV (100 μ M) to block NMDAR-conducted excitatory postsynaptic currents (EPSCs). The peak amplitude of EPSCs was measured to determine current rectification. The amplitude was measured ranging from –80 mV to +60 mV in 20 mV steps. The peak amplitude of EPSCs at –80 mV and +60 mV was measured for the rectification index. In the EPSC ratio experiments, neurons were measured at –80 mV to record AMPAR-EPSCs and were measured at +60 mV to record NMDAR-EPSCs. To determine the AMPAR-to-NMDAR ratio, we measured the peak amplitude of EPSCs at –80 mV as AMPAR-currents and the peak amplitude of EPSCs at +60 mV at 70 ms as NMDAR-currents after onset. For whole-cell LTP recordings, high-frequency stimulation (HFS; 100 Hz, 1 s) was used to induce LTP. For the OGD-induced LTP experiments, the test pulse was delivered regularly during 3 min of OGD incubation. The OGD solution was then rapidly washed out by normal ACSF, and we continued to record EPSCs for 1–2 h. The paired acid injection and test pulse were repeated 3 times with a 20-s interval. Data were acquired at 10 kHz using Multiclamp 700B and pClamp 10.1. The mEPSC events (>5 pA) were analyzed in Clampfit 10. The mEPSC decay time (τ) was fitted to an exponential using Clampfit 10.

2.4. Tail Suspension and Forced Swimming Tests

The tail suspension test and forced swimming test are commonly used in preclinical research to model and study aspects of depression and related conditions, and they are often associated with the concepts of behavioral despair and stress. These tests may indirectly relate to anxiety, given the complex and interconnected nature of depression and anxiety in both preclinical models and clinical conditions [23–25]. ET-1-induced focal ischemia and cannula implantation on day 0. Prepare an ET-1 solution with a concentration of 2 µg/µL by diluting ET-1 in a sterile saline solution (saline solution as the sham control). Ensure proper handling and storage to maintain the solution's integrity. Anesthetize experimental mice using a VetFlo Isoflurane vaporizer throughout the surgery. Ensure proper depth of anesthesia throughout the procedure. For the ET-1 injection and cannula implantation, use stereotaxic coordinates to guide the injection of the ET-1 solution (1 µL each side) into the dual mPFC. Simultaneously, implant a cannula (properly sized for infusion) into the same mPFC region for later drug delivery. For PcTx-1 treatment, for the behavioral tests on day 14, prepare a PcTx-1 solution with a concentration of 100 nM by diluting PcTx-1 in a sterile saline solution. Prepare a separate saline solution as a control. Administer either PcTx-1 or saline solution into the dual amygdala through the implanted cannula. Allow 90 min for the drug to take effect and reach its peak activity. Conduct the tail suspension test to assess depressive-like behaviors. Suspend the mice by their tails using adhesive tape in a controlled environment. Record and analyze the duration of immobility during a predetermined time period. The state of immobility is defined by the absence of movement, except for that which is essential to maintain the subject's nose above water level. The detection of immobility time in these tests serves as a behavioral measure to evaluate the impact of various interventions, such as drug treatments or genetic manipulations, on the animal's response to stress or despair. Conduct the forced swimming test for another group of mice. Place the mice individually in a water-filled container and record their swimming and immobility behaviors. Manually analyze the behavioral results by determining the immobility time for each mouse in both the tail suspension and forced swimming tests. Compile the data and calculate the mean immobility time for each experimental group. Perform an appropriate statistical analysis (e.g., ANOVA) to determine significant differences between groups.

2.5. Statistical Analysis

One-way ANOVA and Tukey's post-hoc multiple comparison tests were used for a statistical comparison of the groups. An unpaired Student's t-test was used to compare results between the two groups. Results were considered statistically significant if $p < 0.05$, and we did not exclude potential outliers from our data except the ones that did not receive successful aversive conditioning. The graphing and statistical analysis software GraphPad Prism 8 was used to analyze statistical data, which was presented as means \pm SEM. Sample sizes (n) are indicated in the figure legends, and data are reported as biological replicates (data from different mice and different brain slices). Each group contained tissues pooled from 4–5 mice. Due to variable behaviors within the groups, we used sample sizes of 10–16 mice per experimental group, as we previously described in earlier experiments [22]. In behavioral studies, we typically studied groups with four randomly assigned animals per group, as our recording equipment allows us to record four separate animal cages simultaneously. The experiments were repeated with another set of four animals until we reached the target number of experimental mice per group. Experimentation groups were repeated in this manner so that each animal had the same controlled environment and the same time of day and similar handling, habituation, and processes.

3. Results

3.1. OGD (In Vitro Ischemia) Enhances ASIC Currents in the Amygdala

To evaluate whether the expression and function of ASICs are correlated with ischemic conditions in the amygdala, we tested the ASIC currents under an in vitro ischemic stroke

condition. OGD, a widely used in vitro model of ischemia, has been shown to increase ASIC currents in cultured cortical neurons [18]. Thus, we examined whether OGD affects ASICs in neurons in the amygdala slices. Amygdala slices were perfused with normal ACSF (bubbled with 5% CO₂ and 95% O₂) or OGD ACSF (bubbled with 5% CO₂ and 95% N₂) for 1 h and then returned to normal ACSF, and the ASIC-like current was activated by a pH 6.0 at −70 mV (Figure 1A). Activation of ASIC currents with a 6.0 pH solution was also performed at indicated time points post-OGD (Figure 1B). Consistent with a previous study, we observed a reduction in ASIC currents during OGD treatment, followed by potentiation after OGD treatment in the amygdala slices. (Figure 1B,C). These data suggested that ASICs might be the main target of brain acidosis in the amygdala after ischemia [18]. We also measured the characteristics of the ASICs after OGD. First, we found the OGD condition leftward drifted the ASIC pH dose-dependent curve to more acidification, and the pH₅₀ was changed from pH₀ 6.4 ± 0.07 to pH₀ 6.2 ± 0.08, $p < 0.001$, suggesting that the component of the ASICs was changed after OGD (Figure 1D). Second, we found the ASIC current desensitization time was prolonged after OGD, supporting the above data that the component of ASICs was changed (Figure 1E). ASIC1a and ASIC2 are the two major ASIC components in the central nervous system, and they form heterozygote-functional ASICs. Previous studies showed that with a lack of ASIC2, the current displays a prolonged current desensitization time and a more acidic pH₅₀ [12,26]. We thus concluded that the OGD condition reduces the ASIC2 proteins in the functional ASICs. To further confirm this conclusion, we tested the ASIC current desensitization time in the ASIC2^{−/−} brain slice before and after OGD. Interestingly, no more change in the desensitization time was found in the ASIC2^{−/−} brain slice, supporting the hypothesis that OGD changes the dynamics of the functional ASICs by reducing the ASIC2 percentage (Figure 1F). The extended inactivation time suggests that the total ASIC-conducted ion influx (Na⁺ and Ca²⁺) per unit time was increased in the neurons from ASIC2^{−/−} mice, resulting in enhanced neuronal activity.

3.2. OGD (In Vitro Ischemia) Enhances ASIC1a-Dependent Synaptic Transmission in the Amygdala

In addition to our investigation of acid-induced ASIC currents, we embarked on an exploration of ASIC1a-dependent excitatory postsynaptic currents (ASIC1a-EPSCs) in response to ischemic conditions (Figure 2A). Building upon our previous data that highlighted H⁺ as an activator of ASIC1a-EPSCs in the amygdala, our findings introduced the intriguing possibility that H⁺ and ASIC1a receptors could potentially serve as a neurotransmitter—receptor pair—regulating critical neuronal communication. Guided by this notion, we formulated the hypothesis that transient OGD might bolster the strength of ASIC1a-EPSCs. To evaluate this hypothesis, we employed a strategy involving the inhibition of AMPA receptor (AMPA), NMDA receptor (NMDAR), and GABA receptor (GABAR)-dependent EPSCs using CNQX, D-APV, and PTX cocktails (Figure 2B). Our results demonstrate a noteworthy enhancement of EPSCs following a mere 10 min of OGD, further corroborated by the inhibitory effects of 200 μM amiloride, an ASIC channel antagonist, underscoring the ASIC1a-dependency of these alterations (Figure 2B,C) [12]. Remarkably, we observed that the potentiation of ASIC1a-EPSCs induced by OGD exhibited a time-dependent characteristic, with peak enhancements occurring approximately 30 min post-OGD (Figure 2B,C). This temporal aspect suggests a dynamic process of synaptic modulation in response to ischemic conditions. It also highlights the potential involvement of ASIC1a in mediating the molecular events that lead to this time-dependent strengthening of synaptic transmission.

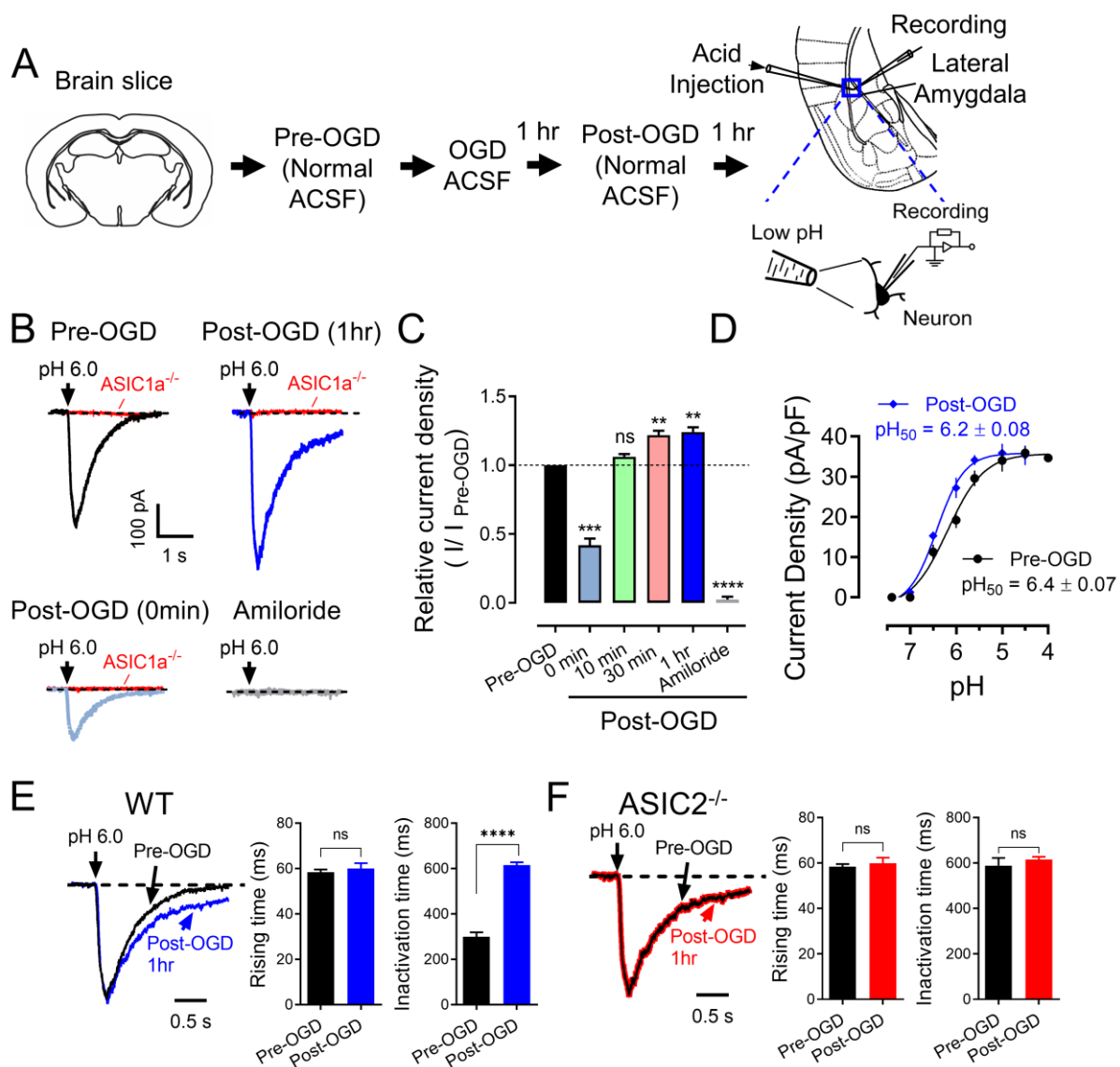


Figure 1. OGD potentiates ASIC1a currents. (A) Representative schematic of protocol for the OGD treatment and ASIC current recordings. (B) The representative traces of pH 6.0-induced currents before and multiple time points after OGD treatment. (C) The summarized data of pH 6.0-induced currents before and after OGD treatment are shown in B. (D) pH-dependent activation of ASIC currents before and after OGD. Best-fit yielded pH_{50} of 6.4 ± 0.07 (pre-OGD) and 6.2 ± 0.08 (post-OGD), $n = 1622$ cells in 4 mice. (E) Normalized acid-induced currents in amygdala slices before and after OGD (black and blue). The decay times in the post-DGD group are longer than in the pre-DGD group, while the rising times remain constant, $n = 19$ cells in 4 mice. (F) Normalized acid-induced currents in $ASIC2^{-/-}$ amygdala slices before and after OGD (black and red), $n = 19$ cells in 4 mice. 'n.s.' indicates not statistically significant. ** $p < 0.01$, *** $p < 0.001$, **** $p < 0.0001$, by unpaired Student's t -test and one-way ANOVA with Tukey's post-hoc multiple comparisons. Data are mean \pm SEM.

Our findings additionally extended into the realm of glutamate receptor (GluR)-dependent EPSCs, which play a central role in synaptic communication. Drawing from previous research indicating that the ratio of AMPA/NMDA EPSCs serve as an indicator of synaptic strength [27], we set out to discern how OGD influences this ratio. Encouragingly, our data revealed an augmented AMPA/NMDA ratio in brain slices subjected to OGD incubation, reflecting an overall strengthening of the synapses (Figure 2D). Importantly, this augmentation was noticeably diminished in the $ASIC1a^{-/-}$ slices, providing strong

evidence for ASIC1a's active participation in regulating these OGD-induced changes (Figure 2E).

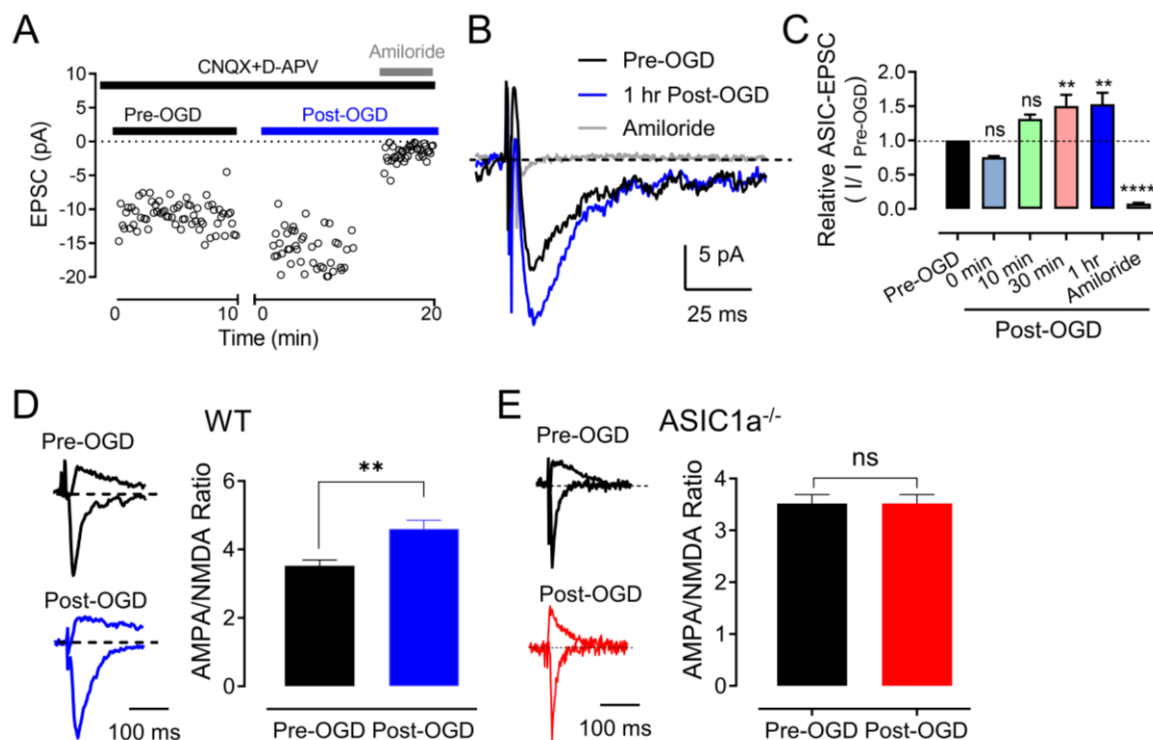


Figure 2. OGD potentiates ASIC1a-dependent EPSCs. (A) ASIC1a-dependent EPSC recordings in amygdala slices. To induce the ASIC1a-dependent EPSCs, test pulses (100 μ s, 0.1 Hz) were delivered through extracellular bipolar electrodes placed on the cortical input. Slices were perfused with 25 μ M CNQX, 50 μ M D-APV, and 100 μ M PTX to eliminate the GluR-dependent EPSCs. The ASIC channel antagonist, 200 μ M of amiloride, was applied during the times indicated. (B) Representative ASIC1a-EPSCs from amygdala slices before and after OGD incubation. (C) The summarized data of the time-dependent ASIC1a-EPSCs before and after OGD incubation shown in B. $n = 4$ –8 slices in 4 mice. ‘n.s.’ indicates not statistically significant. ** $p < 0.01$, **** $p < 0.0001$, by one-way ANOVA with Tukey’s post-hoc multiple comparisons. (D) Left, representative GluR-dependent EPSCs were recorded at -80 mV (AMPA-EPSCs) and $+60$ mV (NMDAR-EPSCs) in WT amygdala slices. Right, the summarized data of AMPA/NMDA ratios. Current amplitudes were measured 70 ms after onset. $n = 15$ slices in 4 mice for each group. (E) The AMPA/NMDA ratios from ASIC1a^{-/-} amygdala slices. $n = 15$ slices in 4 mice for each group. ‘n.s.’ indicates not statistically significant. ** $p < 0.01$, **** $p < 0.0001$, by unpaired Student’s *t*-test. Data are mean \pm SEM.

The observed enhancement of ASIC1a-EPSCs, the time-dependent potentiation, and the alteration in the AMPA/NMDA ratio collectively imply that OGD-induced changes might recalibrate the efficiency of synaptic communication in the amygdala. Given that ASIC1a is implicated in mediating these synaptic adjustments, the study underscores the pivotal role of this receptor in the context of ischemia-induced alterations in neurotransmission.

3.3. ASIC1a Contributes to OGD-Induced LTP

Building upon the existing scientific literature that has documented the emergence of OGD-induced immediate LTP, indicating the potential contribution of heightened synaptic functionality in the aftermath of pathological conditions such as brain ischemia [28], we delved deeper into this intriguing phenomenon. Our investigation employed a cohort of WT mice subjected to a concise 3 min episode of OGD to unravel the dynamics of LTP under these conditions (Figure 3A). The results yielded a remarkable outcome, revealing the establishment of robust LTP, with the recorded measurements surging to $148 \pm 2\%$ of

the pre-OGD baseline ($n = 10, p < 0.05$). This finding underscores the potential for rapid synaptic strengthening in response to OGD, further suggesting a compensatory mechanism is at play to counteract the adverse effects of ischemic insults. However, this landscape exhibited significant alterations when examining the $ASIC1a^{-/-}$ mice. In this context, the absence of $ASIC1a$ led to the complete annulment of OGD-induced LTP, evident from the recorded values plateauing at $103 \pm 5\%$ of the pre-OGD baseline ($n = 8, p > 0.05$; Figure 3B).

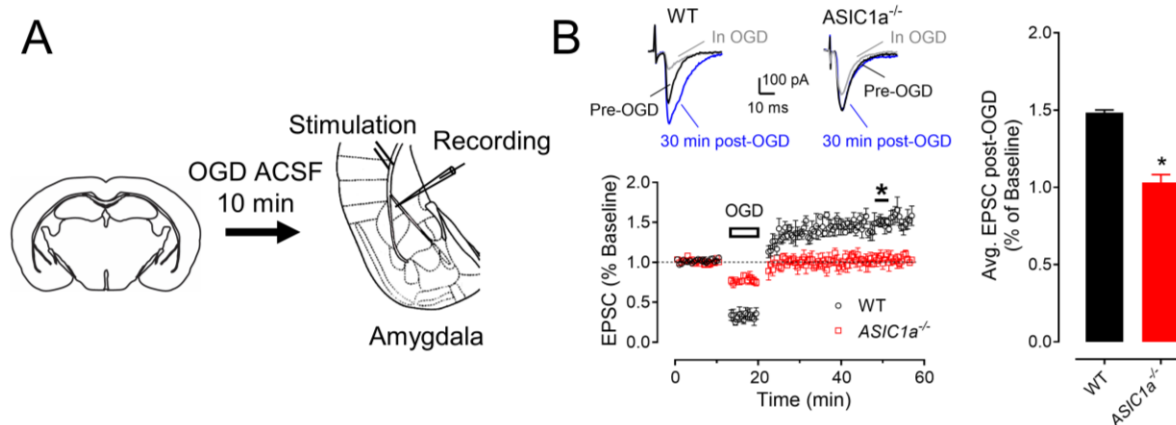


Figure 3. OGD-induced ischemic-LTP in amygdala brain slices. (A) LTP after OGD (black trace). Top: representative EPSC traces, pre-OGD, OGD, and 30 min after OGD, as indicated. Bottom: EPSCs were recorded in normal ACSF for 10 min as a baseline, and then the slice was perfused with OGD for 3 min and then returned to normal ACSF. Note: EPSCs were not enhanced after OGD in $ASIC1a^{-/-}$ amygdala slices (red trace). (B) Summarized data showing relative EPSCs 30 min after OGD. $n = 4$ slices in 4 mice for each group. * $p < 0.05$, by unpaired Student's t -test. Data are mean \pm SEM.

This striking dichotomy in OGD-induced LTP responses provides a direct glimpse into the pivotal role of $ASIC1a$ in mediating the immediate synaptic potentiation that follows OGD. It highlights $ASIC1a$ as a critical molecular entity orchestrating the rapid adaptive changes in synaptic strength in the wake of ischemic challenges.

3.4. In Vivo Ischemia Enhances ASIC Currents and Neuronal Activities in the Amygdala

We employed two distinct in vivo mouse models of ischemia to investigate the effects of focal cerebral ischemia on amygdala neuronal activity and synaptic plasticity. The first model utilized endothelin-1 (ET-1), a vasoconstrictor peptide, to induce focal ischemia within the mPFC [29,30]. A single injection of 1.0 μ g of ET-1 or saline (sham group) was administered in the mPFC, with coordinates relative to the bregma set at +2.0 mm anterior—posterior, +0.5 mm mediolateral, and -2.4 mm dorsoventral. Subsequently, we explored whether this focal ischemic insult in the mPFC had any impact on ASIC currents within amygdala neurons. Two days following the ET-1 injection, we sacrificed the animals and prepared amygdala slices for patch-clamp recordings (Figure 4A). The efficacy of the ET-1-induced ischemia in the mPFC was confirmed using crystal violet staining, revealing a distinct ischemic site (Figure 4B). We then assessed the ASIC currents through activation with a 4.5 pH solution at specific time points. In alignment with prior research indicating that cerebral ischemia enhances ASIC currents [31], we observed a robust potentiation of ASIC-like currents within the amygdala slices subsequent to ET-1-induced ischemia in the PFC (Figure 4C). These findings suggest the potential involvement of $ASIC1a$ in mediating alterations within the PFC-amygdala circuit under ischemic conditions.

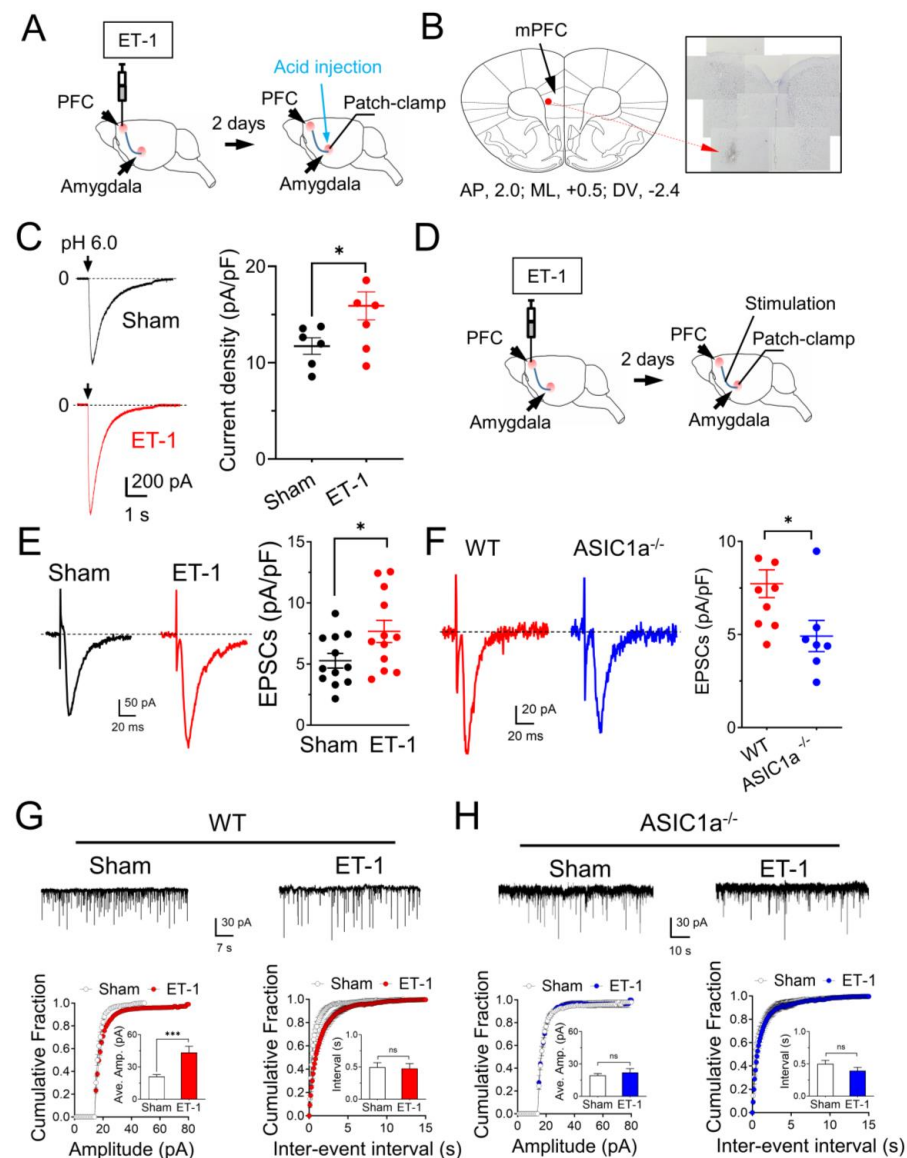


Figure 4. ET-1-induced ischemia in the mPFC potentiates ASIC1a currents and EPSCs in the amygdala. (A) Representative schematic of protocol for ET-1 injection and ASIC current recordings. (B) Example image of crystal violet staining showing the ET-1-induced ischemia in the mPFC. (C) Representative traces (left) and summarized data (right) of pH 6.0-induced currents in the amygdala before and after ET-1 injection in the mPFC. $n = 6$ cells in 4 mice. (D) Representative schematic of protocol for ET-1 injection and EPSC recordings. (E) Representative traces (left) and summarized data (right) of EPSCs in the amygdala before and after ET-1 injection in the mPFC. $n = 12$ cells in 4 mice. (F) Representative traces (left) and summarized data (right) of EPSCs in the amygdala after ET-1 injection in the WT and ASIC1a^{-/-} mPFC, respectively. $n = 8$ cells in 4 mice. (G) Upper, representative mEPSC traces in the sham and ET-1 injection groups; lower, cumulative distributions of mEPSC amplitudes and inter-event intervals in the sham (black) and ET-1 injection (red) WT mice. Insets are the summarized data of amplitudes and inter-event intervals. (H) The mEPSC results in the sham (black) and ET-1 injection (blue) ASIC1a^{-/-} mice. ‘n.s.’ indicates not statistically significant. * $p < 0.01$, *** $p < 0.0001$, by unpaired Student’s *t*-test. Data are mean \pm SEM.

Expanding our investigations, we explored the influence of mPFC ischemia on EPSCs within the amygdala. Following a two-day interval post-ET-1 injection, we sacrificed the animals and conducted evoked EPSC recordings by stimulating cortical inputs and examining miniature EPSCs (mEPSCs) (Figure 4D). Remarkably, we observed a signifi-

cant potentiation of EPSCs in the amygdala slices following ET-1-induced ischemia in the mPFC (Figure 4E), consistent with previously documented ischemia-induced EPSC enhancements [32]. Interestingly, this scenario was notably altered in mice with an ASIC1a deficiency within the amygdala slices (Figure 4F). Similar findings were observed in the mEPSC recordings, where we discovered that ET-1-induced ischemia in the mPFC increased the mEPSC amplitude in the amygdala (Figure 4G), however this increase was abrogated in the ASIC1a^{-/-} amygdala slices (Figure 4H).

3.5. The mPFC Ischemia-Induced Depression-like Behaviors Are ASICs-Dependent

Utilizing the ET-1 ischemia mouse model, we established a focused ischemic infarction within the mPFC to investigate emotional behaviors reliant on the amygdala (Figure 5A). In particular, we explored depression-like behaviors through the implementation of two distinct paradigms (Figure 5B). The tail suspension test (TST), recognized as an established method for assessing stress and depression in rodents [33], measures immobility as an indicator of helplessness. Notably, our findings revealed an increased duration of immobility in mice injected with ET-1 within the PFC group as compared to the sham group (Figure 5C). This observation strongly supports the hypothesis that focal ischemia within the PFC exacerbates depressive-like behaviors, with the involvement of the amygdala in this phenomenon. To further scrutinize depressive-like behaviors, we employed the force swimming test (FST), another well-regarded measure of depressive-like tendencies [25]. The injection of the mPFC groups with ET-1 led to a significant elevation in the time of immobility when contrasted with the sham-treated group (Figure 5D). Collectively, these data indicate that targeted ischemia within the PFC has the capacity to induce a state of depressive-like behavior, offering insight into the complex interactions between brain regions in emotional regulation.

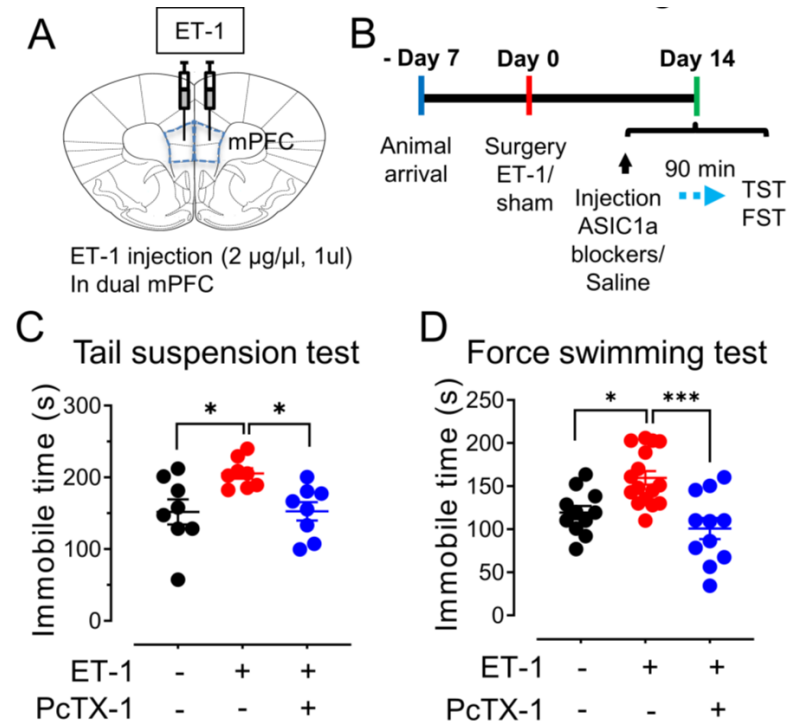


Figure 5. ET-1-induced focal ischemia in the mPFC potentiates depression-like behaviors. (A) Schematic of protocol for ET-1 injection in dual mPFC. (B) Representative schematic of behavioral

paradigm. (C) The summarized results of the tail suspension test. The injection of 1 μ M ET-1 and 100 nM PcTx-1 are indicated in B. $n = 8$ mice in each group. (D) The summarized results of the forced swimming test. $n = 11$ –16 mice in each group. * $p < 0.05$, *** $p < 0.001$, by one-way ANOVA with Tukey's post-hoc multiple comparisons. Data are mean \pm SEM.

To elucidate the role of the ASIC1a subunit in these anxiety- and depression-like behaviors, we administered a specific ASIC1a blocker, 100 μ M PcTx-1, 90 min prior to the commencement of the behavioral tests, encompassing both TST and FST. Intriguingly, our results indicate that the suppression of ASIC1a through PcTx-1 administration yields a substantial reduction in the exacerbated immobility observed in both TST and FST in the context of mPFC ischemia (Figure 5C,D). This finding lends compelling support to the premise that the manifestation of depression-like behaviors induced by ET-1-driven ischemia within the mPFC is intricately linked to the presence of ASIC1a. By selectively blocking ASIC1a, we observe a mitigation of these behaviors, implying a pivotal role for this ion channel subunit in influencing the emotional response to ischemic insults.

4. Discussion

Understanding the molecular mechanisms that underlie neuron dysfunction after a stroke is crucial for developing effective neuroprotective strategies. Cerebral ischemia is a major cause of stroke, which leads to neuronal deficits and brain damage. A dysfunction of synaptic activity is the earliest consequence of cerebral ischemia [34]. Elucidating the connections between ischemia and synaptic transmission and plasticity is a key step to understanding and preventing neuron dysfunction after a stroke. We hypothesize that ASIC1a is an important therapeutic target that may be modulated to protect against neuronal deficits caused by an ischemic stroke and post-stroke mental disorders. The results of our study provide a comprehensive exploration of the impact of in vitro and in vivo ischemic conditions on the function of ASICs and their associated synaptic activity in the amygdala. The role of ASICs in mediating neuronal responses under ischemic conditions has been elucidated, shedding light on their potential contributions to pathological alterations in neural circuits, synaptic plasticity, and behavioral outcomes.

Our investigation into the effect of in vitro ischemia on ASIC currents in the amygdala yielded compelling results. This finding underscores the significance of ASICs in responding to ischemic conditions and suggests that they might be central to the alterations in the PFC-amygdala circuit following ischemic events. Additionally, we observed changes in the characteristics of ASIC currents after OGD, including a shift in the pH dependence and prolonged desensitization time. The results provide strong evidence that ischemic conditions significantly impact ASIC currents in the amygdala. The observed potentiation of ASIC currents following OGD aligns with previous reports in cortical neurons [18,32], indicating a broader role of ASICs in responding to ischemia. The pronounced increase in ASIC currents following OGD suggests that these channels are highly sensitive to ischemic events. This is further supported by the altered pH sensitivity of ASICs after OGD, with the leftward shift of the pH dose-response curve and prolonged desensitization time. These changes point towards a dynamic remodeling of ASIC properties under ischemic conditions, possibly involving alterations in the channel subunit composition.

This study delves into the ASIC1a-EPSCs and their modulation by OGD. The enhanced ASIC1a-EPSCs following transient OGD suggest that ASIC-mediated H^+ signaling plays a role in strengthening synaptic transmission [32]. Notably, the time-dependent increase in ASIC1a-EPSCs after OGD highlights a potential mechanism for prolonged synaptic potentiation, which may have implications for information processing and plasticity in the amygdala. The findings related to the AMPAR/NMDAR ratio further underscore the impact of ASICs on glutamate receptor-mediated synaptic transmission. The increase in the AMPAR/NMDAR ratio after OGD suggests an enhanced synaptic strength, which aligns with previously established markers of potentiated synapses [27]. The diminished difference in the AMPAR/NMDAR ratio in the ASIC1a^{-/-} slices strengthens the case for ASIC1a's involvement in these changes. This finding extends our understanding of

ASICs beyond their direct H⁺-gated currents to their modulation of glutamate receptor-mediated signaling, indicating a more complex role in synaptic function. The discovery of OGD-induced LTP provides a novel perspective on the interplay between ischemic events and synaptic plasticity. The observed robust LTP following brief OGD exposure suggests that a heightened synaptic function under pathological conditions contributes to delayed consequences of brain ischemia, potentially influencing long-term outcomes. Importantly, the significant attenuation of LTP in ASIC1a-deficient mice highlight ASIC1a's pivotal role in mediating this phenomenon. This finding underscores the significance of ASIC1a in influencing synaptic plasticity dynamics in response to ischemic challenges.

The transition to *in vivo* ischemia models brings the study closer to the physiological context of brain ischemia. The investigation into ASIC currents and evoked EPSCs following focal ischemia in the mPFC provides evidence for enhanced neural activities in the amygdala. The potentiation of ASIC-like currents following ET-1 injection further emphasizes the role of ASIC1a in mediating the alterations of the PFC-amygdala circuitry in response to ischemic events. This aligns with reports of changes in emotional, memory, and behavioral functions following cerebral ischemia. The implications of this study extend beyond synaptic changes to emotional behaviors. The ET-1-induced focal ischemia in the mPFC results in depression-like behaviors, as evidenced by increased immobility times in the TST and FST tests. The correlation between focal ischemia and depressive behaviors highlights the potential impact of ischemia on emotional regulation. The rescue of these behaviors by the ASIC1a blocker PcTX-1 indicates ASIC1a's involvement in mediating the effects of ischemia on emotional states.

While this study significantly advances our understanding of ASICs in the context of ischemia, it also raises intriguing questions and potential avenues for future research. Further investigation into the downstream signaling pathways triggered by ASIC activation, the involvement of ASICs in network-wide effects of ischemia, and their role in long-term consequences would provide a more complete picture. Additionally, exploring the potential cross-talk between ASICs and other ion channels and receptors could uncover complex interactions underlying the observed changes.

5. Conclusions

In conclusion, these results provide critical insights into the roles of ASICs in mediating synaptic plasticity changes and emotional responses under ischemic challenges. This study in mice provides a foundation for understanding the impact of ischemia on ASIC1a function in the amygdala and its potential implications for synaptic plasticity and emotional behaviors. While a direct extrapolation of human stroke requires further investigation, the findings contribute to our broader understanding of the molecular and neural mechanisms involved in ischemic events. The findings open up new avenues for future research and potential therapeutic interventions targeting ASICs to ameliorate the effects of ischemia on brain function and emotional well-being.

Author Contributions: J.D. conceived the project. J.D., G.P., Q.G. and Z.J. designed the experiments. G.P. and J.D. performed the patch-clamp experiments and data analysis. Q.G. and Z.J. performed the behavior experiments and data analysis. G.P., Q.G. and Z.J. contributed equally to this paper. All authors reviewed and edited the manuscript. All authors have read and agreed to the published version of the manuscript.

Funding: This work was funded by American Heart Association (15SDG25700054) and National Institutes of Mental Health (1R01MH113986).

Institutional Review Board Statement: The animal study protocol was approved by the Institutional Review Board of The University of Tennessee Health Science Center Laboratory Animal Care Unit (Protocol #19-0112, approval date 15 January 2020) and the University of Toledo Institutional Animal Care and Use Committee (Protocol #108791, approval date 28 October 2016).

Data Availability Statement: All of the data analyzed in this study are publicly available and on reasonable request from the corresponding author.

Acknowledgments: We appreciate Michael Welsh and Joh Wemmie for providing the ASIC1a and ASIC2 mice. We also appreciate our previous lab members, Fara Naghavi and Mitchell Silvernail for their assistance.

Conflicts of Interest: The authors declare no conflict of interest.

References

1. Hackett, M.L.; Kohler, S.; O'Brien, J.T.; Mead, G.E. Neuropsychiatric outcomes of stroke. *Lancet Neurol.* **2014**, *13*, 525–534. [[CrossRef](#)] [[PubMed](#)]
2. Murphy, T.H.; Corbett, D. Plasticity during stroke recovery: From synapse to behaviour. *Nat. Rev. Neurosci.* **2009**, *10*, 861–872. [[CrossRef](#)] [[PubMed](#)]
3. Xerri, C.; Zennou-Azogui, Y.; Sadlaoud, K.; Sauvajon, D. Interplay between intra- and interhemispheric remodeling of neural networks as a substrate of functional recovery after stroke: Adaptive versus maladaptive reorganization. *Neuroscience* **2014**, *283*, 178–201. [[CrossRef](#)] [[PubMed](#)]
4. Naghavi, F.S.; Koffman, E.E.; Lin, B.; Du, J. Post-stroke neuronal circuits and mental illnesses. *Int. J. Physiol. Pathophysiol. Pharmacol.* **2019**, *11*, 1–11. [[PubMed](#)]
5. Janak, P.H.; Tye, K.M. From circuits to behaviour in the amygdala. *Nature* **2015**, *517*, 284–292. [[CrossRef](#)] [[PubMed](#)]
6. Cheng, B.; Forkert, N.D.; Zavaglia, M.; Hilgetag, C.C.; Golsari, A.; Siemonsen, S.; Fiehler, J.; Pedraza, S.; Puig, J.; Cho, T.H.; et al. Influence of stroke infarct location on functional outcome measured by the modified rankin scale. *Stroke* **2014**, *45*, 1695–1702. [[CrossRef](#)] [[PubMed](#)]
7. Rehncrona, S. Brain acidosis. *Ann. Emerg. Med.* **1985**, *14*, 770–776. [[CrossRef](#)]
8. Siesjo, B.K.; Katsura, K.; Kristian, T. Acidosis-related damage. *Adv. Neurol.* **1996**, *71*, 209–233.
9. Nedergaard, M.; Kraig, R.P.; Tanabe, J.; Pulsinelli, W.A. Dynamics of interstitial and intracellular pH in evolving brain infarct. *Am. J. Physiol.* **1991**, *260*, R581–R588. [[CrossRef](#)]
10. Siesjo, B.K. Acidosis and ischemic brain damage. *Neurochem. Pathol.* **1988**, *9*, 31–88. [[CrossRef](#)]
11. Choi, D.W. Calcium: Still center-stage in hypoxic-ischemic neuronal death. *Trends Neurosci.* **1995**, *18*, 58–60. [[CrossRef](#)] [[PubMed](#)]
12. Du, J.; Reznikov, L.R.; Price, M.P.; Zha, X.M.; Lu, Y.; Moninger, T.O.; Wemmie, J.A.; Welsh, M.J. Protons are a neurotransmitter that regulates synaptic plasticity in the lateral amygdala. *Proc. Natl. Acad. Sci. USA* **2014**, *111*, 8961–8966. [[CrossRef](#)] [[PubMed](#)]
13. Coryell, M.W.; Wunsch, A.M.; Haenfler, J.M.; Allen, J.E.; Schnizler, M.; Ziemann, A.E.; Cook, M.N.; Dunning, J.P.; Price, M.P.; Rainier, J.D.; et al. Acid-sensing ion channel-1a in the amygdala, a novel therapeutic target in depression-related behavior. *J. Neurosci.* **2009**, *29*, 5381–5388. [[CrossRef](#)] [[PubMed](#)]
14. Wemmie, J.A.; Coryell, M.W.; Askwith, C.C.; Lamani, E.; Leonard, A.S.; Sigmund, C.D.; Welsh, M.J. Overexpression of acid-sensing ion channel 1a in transgenic mice increases acquired fear-related behavior. *Proc. Natl. Acad. Sci. USA* **2004**, *101*, 3621–3626. [[CrossRef](#)] [[PubMed](#)]
15. Coryell, M.W.; Ziemann, A.E.; Westmoreland, P.J.; Haenfler, J.M.; Kurjakovic, Z.; Zha, X.M.; Price, M.; Schnizler, M.K.; Wemmie, J.A. Targeting ASIC1a reduces innate fear and alters neuronal activity in the fear circuit. *Biol. Psychiatry* **2007**, *62*, 1140–1148. [[CrossRef](#)]
16. Waldmann, R.; Champigny, G.; Bassilana, F.; Heurteaux, C.; Lazdunski, M. A proton-gated cation channel involved in acid-sensing. *Nature* **1997**, *386*, 173–177. [[CrossRef](#)]
17. Waldmann, R.; Lazdunski, M. H(+)-gated cation channels: Neuronal acid sensors in the NaC/DEG family of ion channels. *Curr. Opin. Neurobiol.* **1998**, *8*, 418–424. [[CrossRef](#)]
18. Xiong, Z.G.; Zhu, X.M.; Chu, X.P.; Minami, M.; Hey, J.; Wei, W.L.; MacDonald, J.F.; Wemmie, J.A.; Price, M.P.; Welsh, M.J.; et al. Neuroprotection in ischemia: Blocking calcium-permeable acid-sensing ion channels. *Cell* **2004**, *118*, 687–698. [[CrossRef](#)]
19. Chesler, M. Regulation and modulation of pH in the brain. *Physiol. Rev.* **2003**, *83*, 1183–1221. [[CrossRef](#)]
20. Takmakov, P.; Zachek, M.K.; Keithley, R.B.; Bucher, E.S.; McCarty, G.S.; Wightman, R.M. Characterization of local pH changes in brain using fast-scan cyclic voltammetry with carbon microelectrodes. *Anal. Chem.* **2010**, *82*, 9892–9900. [[CrossRef](#)]
21. Kai Kaila, B.R.R. *pH and Brain Function*, 1st ed.; Wiley-Liss: New York City, NY, USA, 1998; p. 688.
22. Du, J.; Price, M.P.; Taugher, R.J.; Grigsby, D.; Ash, J.J.; Stark, A.C.; Hossain Saad, M.Z.; Singh, K.; Mandal, J.; Wemmie, J.A.; et al. Transient acidosis while retrieving a fear-related memory enhances its lability. *eLife* **2017**, *6*, e22564. [[CrossRef](#)] [[PubMed](#)]
23. Bielajew, C.; Konkle, A.T.; Kentner, A.C.; Baker, S.L.; Stewart, A.; Hutchins, A.A.; Santa-Maria Barbagallo, L.; Fouriez, G. Strain and gender specific effects in the forced swim test: Effects of previous stress exposure. *Stress* **2003**, *6*, 269–280. [[CrossRef](#)] [[PubMed](#)]
24. Fujisaki, C.; Utsuyama, M.; Kuroda, Y.; Watanabe, A.; Seidler, H.; Watanabe, S.; Kitagawa, M.; Hirokawa, K. An immunosuppressive drug, cyclosporine-A acts like anti-depressant for rats under unpredictable chronic stress. *J. Med. Dent. Sci.* **2003**, *50*, 93–100. [[PubMed](#)]
25. Yankelevitch-Yahav, R.; Franko, M.; Huly, A.; Doron, R. The forced swim test as a model of depressive-like behavior. *J. Vis. Exp.* **2015**, *97*, e52587. [[CrossRef](#)]
26. Askwith, C.C.; Wemmie, J.A.; Price, M.P.; Rokhlina, T.; Welsh, M.J. Acid-sensing ion channel 2 (ASIC2) modulates ASIC1 H⁺-activated currents in hippocampal neurons. *J. Biol. Chem.* **2004**, *279*, 18296–18305. [[CrossRef](#)]

27. Rao, V.R.; Finkbeiner, S. NMDA and AMPA receptors: Old channels, new tricks. *Trends Neurosci.* **2007**, *30*, 284–291. [[CrossRef](#)]
28. Calabresi, P.; Saulle, E.; Centonze, D.; Pisani, A.; Marfia, G.A.; Bernardi, G. Post-ischaemic long-term synaptic potentiation in the striatum: A putative mechanism for cell type-specific vulnerability. *Brain* **2002**, *125*, 844–860. [[CrossRef](#)]
29. Horie, N.; Maag, A.L.; Hamilton, S.A.; Shichinohe, H.; Bliss, T.M.; Steinberg, G.K. Mouse model of focal cerebral ischemia using endothelin-1. *J. Neurosci. Methods* **2008**, *173*, 286–290. [[CrossRef](#)]
30. Chan, H.H.; Cooperrider, J.L.; Park, H.J.; Wathen, C.A.; Gale, J.T.; Baker, K.B.; Machado, A.G. Crossed Cerebellar Atrophy of the Lateral Cerebellar Nucleus in an Endothelin-1-Induced, Rodent Model of Ischemic Stroke. *Front. Aging Neurosci.* **2017**, *9*, 10. [[CrossRef](#)]
31. Xiong, Z.G.; Pignataro, G.; Li, M.; Chang, S.Y.; Simon, R.P. Acid-sensing ion channels (ASICs) as pharmacological targets for neurodegenerative diseases. *Curr. Opin. Pharmacol.* **2008**, *8*, 25–32. [[CrossRef](#)]
32. Quintana, P.; Soto, D.; Poirot, O.; Zonouzi, M.; Kellenberger, S.; Muller, D.; Chrast, R.; Cull-Candy, S.G. Acid-sensing ion channel 1a drives AMPA receptor plasticity following ischaemia and acidosis in hippocampal CA1 neurons. *J. Physiol.* **2015**, *593*, 4373–4386. [[CrossRef](#)] [[PubMed](#)]
33. Castagne, V.; Moser, P.; Porsolt, R.D. Behavioral Assessment of Antidepressant Activity in Rodents. In *Methods of Behavior Analysis in Neuroscience*, 2nd ed.; Buccafusco, J.J., Ed.; Frontiers in Neuroscience: Boca Raton, FL, USA, 2009.
34. Hofmeijer, J.; van Putten, M.J. Ischemic cerebral damage: An appraisal of synaptic failure. *Stroke* **2012**, *43*, 607–615. [[CrossRef](#)] [[PubMed](#)]

Disclaimer/Publisher’s Note: The statements, opinions and data contained in all publications are solely those of the individual author(s) and contributor(s) and not of MDPI and/or the editor(s). MDPI and/or the editor(s) disclaim responsibility for any injury to people or property resulting from any ideas, methods, instructions or products referred to in the content.